Geomorphology xxx (2012) xxx

Contents lists available at SciVerse ScienceDirect

Geomorphology

journal homepage: www.elsevier.com/locate/geomorph

Highlights

Geomorphology xxx (2012) xxx–xxx

Reconstructing palaeo-volcanic geometries using a Geodynamic Regression Model (GRM): Application to Deception Island volcano (South Shetland Islands, Antarctica)

C. Torrecillas [a,*], M. Berrocoso [b], A. Felpeto [c], M.D. Torrecillas [a], A. Garcia [d]

[a] Escuela Tecnica Superior de Ingenieros, University of Seville, Av. De los Descubrimientos s/n, 41092 Seville, Spain
[b] Facultad de Ciencias, University of Cadiz, Campus Puerto Real, 11510, Puerto Real, Cadiz, Spain
[c] Central Geophysical Observatory, Spanish Geographic Institute, Alfonso XII, 3, 28014 Madrid, Spain
[d] Departamento de Volcanologia, Museo Nacional de Ciencias Naturales, C/Jose Gutierrez Abascal, 2, 28006 Madrid, Spain

► Reconstruction of an island previous to the formation of its caldera is proposed. ► Input data: topography, bathymetry, pre-caldera deposits and deformation rates. ► Taken into account: mass balance due to ice, erosion and sea level. ► The palaeo-summit height calculated for the palaeo-stratovolcano is 640 m. ► The method reveals the pre-existence of parasite volcanoes.

http://dx.doi.org/10.1016/j.geomorph.2012.10.032

Geomorphology xxx (2012) xxx–xxx

Contents lists available at SciVerse ScienceDirect

Geomorphology

journal homepage: www.elsevier.com/locate/geomorph

Reconstructing palaeo-volcanic geometries using a Geodynamic Regression Model (GRM): Application to Deception Island volcano (South Shetland Islands, Antarctica)

C. Torrecillas [a,*], M. Berrocoso [b], A. Felpeto [c], M.D. Torrecillas [a], A. Garcia [d]

[a] Escuela Tecnica Superior de Ingenieros, University of Seville, Av. De los Descubrimientos s/n, 41092 Seville, Spain
[b] Facultad de Ciencias, University of Cadiz, Campus Puerto Real, 11510, Puerto Real, Cadiz, Spain
[c] Central Geophysical Observatory, Spanish Geographic Institute, Alfonso XII, 3, 28014 Madrid, Spain
[d] Departamento de Volcanologia, Museo Nacional de Ciencias Naturales, C/Jose Gutierrez Abascal, 2, 28006 Madrid, Spain

ARTICLE INFO

Article history:
Received 6 May 2011
Received in revised form 25 October 2012
Accepted 27 October 2012
Available online xxxx

Keywords:
Palaeo-volcano
Palaeo-surface
Terrain reconstruction
Volcanic deformation
Digital elevation model

ABSTRACT

This article describes a reconstruction made of the palaeo-volcanic edifice on Deception Island (South Shetland Islands, Antarctica) prior to the formation of its present caldera. Deception Island is an active Quaternary volcano located in the Bransfield Strait, between the South Shetland Islands and the Antarctic Peninsula. The morphology of the island has been influenced mainly by the volcanic activity but geodynamics and volcanic deformation have also contributed. A volcanic reconstruction method, the Geodynamic Regression Model (GRM), which includes a terrain deformation factor, is proposed. In the case of Deception Island, the directions of this deformation are NW–SE and NE–SW, and match both the observed deformation of the Bransfield Strait and the volcanic deformation monitored over the last 20 years in the island, using Global Navigation Satellite System (GNSS) techniques. Based on these data, possible volcanic deformation values of 5–15 mm/yr in these directions have been derived. A possible coastline derived from a current bathymetry is transformed, according to values for the chosen date, to obtain the palaeo-coastline of Deception Island of 100 k years ago. Topographic, geomorphologic, volcanological and geological data in a GIS system have been considered, for computation of the outside caldera slope, palaeo-coastline, palaeo-summit height and palaeo digital elevation model (DEM). The result is a 3D palaeo-geomorphological surface model of a volcano, reaching 640 m in height, with an increase of 4 km^3 in volume compared to the current edifice, covering 4 km^2 more surface area and the method reveals the previous existence of parasite volcanoes. Two photorealistic images of the island are obtained by superposition of textures extracted from a current Quick Bird satellite image also. This technique for reconstructing the terrain of an existing volcano could be useful for analysing the past and future geomorphology of this island and similar locations.

1. Introduction

Many volcanic processes, including caldera formation and sector collapses, may drastically change the early morphology of volcanic edifices. Although the reconstruction of these early morphologies is complex, 3D software and GIS technology allow reconstruction of the palaeo-topography of volcanoes. Different parameters need to be deduced for the size and shape of old edifices. Szekely and Karatson (2004), using parameters derived from a digital elevation model (DEM), infer the original shape of highly-degraded volcanic structures in the Börzsöny Mountains (Hungary). Rodriguez et al. (2004) proposed a reconstruction of a volcanic edifice in Paipa (Colombia) using pyroclastic deposits and 3D software to model flows. Rodriguez-Gonzalez et al. (2010) described a methodology for reconstructing the volcanic landform prior to a monogenetic basaltic eruption in El Lentiscal (Canary Islands, Spain), modelling both the scoria cone and the lava flow using morphometric modelling from the present-day DEM. Other methodologies for reconstructing original surfaces use inward extrapolation of the mean slope to define the main conic centre and height, and kriging with linear variograms as method of interpolation (Hildenbrand et al., 2008). Vogel and Marker (2010) reconstructed areas from the thicknesses of identified layers and then interpolated them with spline functions, as in Coleman et al. (2009) and Isaia et al. (2004), in their computation of the total volume of eruptions of the Astroni volcano (Italy).

The multiplicity of the above methodologies indicates that a standard procedure for the reconstruction of palaeo-volcanic surfaces is still lacking; significantly, none of the proposed methodologies takes into consideration a deformation parameter.

Deception Island is an active Quaternary volcano located in the Bransfield Strait, between the South Shetland Islands and the Antarctic

* Corresponding author at: Departamento de Ingenieria Grafica, Escuela Tecnica Superior de Ingenieros, Av. de los Descubrimientos s/n, 41092 Seville, Spain. Tel.: +34 95448659; fax: +34 954486158.
E-mail addresses: torrecillas@us.es (C. Torrecillas), Manuel.berrocoso@uca.es (M. Berrocoso), afelpeto@fomento.es (A. Felpeto), mtorrecillas@us.es (M.D. Torrecillas), aliciag@mncn.csic.es (A. Garcia).

0169-555X/$ – see front matter
http://dx.doi.org/10.1016/j.geomorph.2012.10.032

Peninsula (Fig. 1). The area is characterised by complex tectonics related to the interaction of two main plates (the South American and Antarctic plates), and three micro-plates (the Scotia, Phoenix (also known as Drake) and South Shetland plates (Baraldo, 1999)). The bathymetric study of the island and the surrounding area indicates that the deformation is due to regional extension across the basin, with local, superimposed effects related to caldera collapse and magma inflation. Due to this geodynamic complexity, the reconstruction of Deception Island palaeo-geometry requires the application of a new methodology, as presented in this study.

The technique of terrain reconstruction described herein can be useful for analysing the past and future geomorphology of the island. The reconstruction of past conditions on this Island may help to clarify its evolution, by establishing whether or not certain geomorphological scenarios are possible, and may give some clues to support or rule out one of the proposed theories on its evolution. Furthermore, the construction of likely scenarios for the near future could contribute to a better evaluation of the volcanic hazard by the identification of the geomorphic features symptomatic of possible instability related to future volcanic eruptions or earthquakes.

2. Methodology

A new method for the reconstruction of palaeo-geometries here applied here to the pre-caldera volcano of Deception Island. This approach can be divided into two distinct and successive stages:

a) In the first stage, the existing remains of the palaeo-surface are extracted, and the relevant geometries of the palaeo-volcano are determined. Data from the geological, topographic, bathymetric and geomorphological maps are fundamental to this stage. Existing hypotheses of the island's geological evolution must be analysed carefully to define peculiar aspects of the shape and surfaces to be reconstructed; these include the palaeo-coastline, the number of the main parasitic volcanoes and their height, and palaeo- or pre-caldera deposits. These data are used to define the most likely palaeo-surface,
b) In the second stage, a Geodynamic Regression Model (GRM) is applied to this palaeo-surface to transform it to a specific time in the past. The regional and local deformation of the volcano surface is studied and quantified to calculate a geometric transformation to the selected time using deformation vectors. The date in the past for this GRM is also established in this stage. Before calculating the final surface, important parameters are estimated, such as the mass balance due to ice, glaciation periods and sea level values, which are potential factors of influence, for re-analysing or re-calculating the volcano's height in the reconstruction. Finally, a DEM is interpolated with the palaeo-data, and the definitive morphology is recreated. To improve the visual aesthetics of the reconstruction, real or postulated surface textures are applied.

2.1. Palaeo-reconstruction of the pre-caldera volcano on Deception Island

2.1.1. Geomorphology and geological evolution of Deception Island

Deception Island (South Shetland Islands, Antarctica) is an emerged volcano less than 780 kyr old (Baraldo et al., 2003) whose geological evolution is marked by the formation of a large, though hitherto undated, central caldera that clearly separates the island's stratigraphy into pre-caldera and post-caldera deposits.

The island has a submerged basal diameter of 30 km, an altitude of 1500 m from the sea bottom (Barclay et al., 2009), and 540 m m.a.s.l. The emerged portion is horseshoe-shaped with a diameter of about

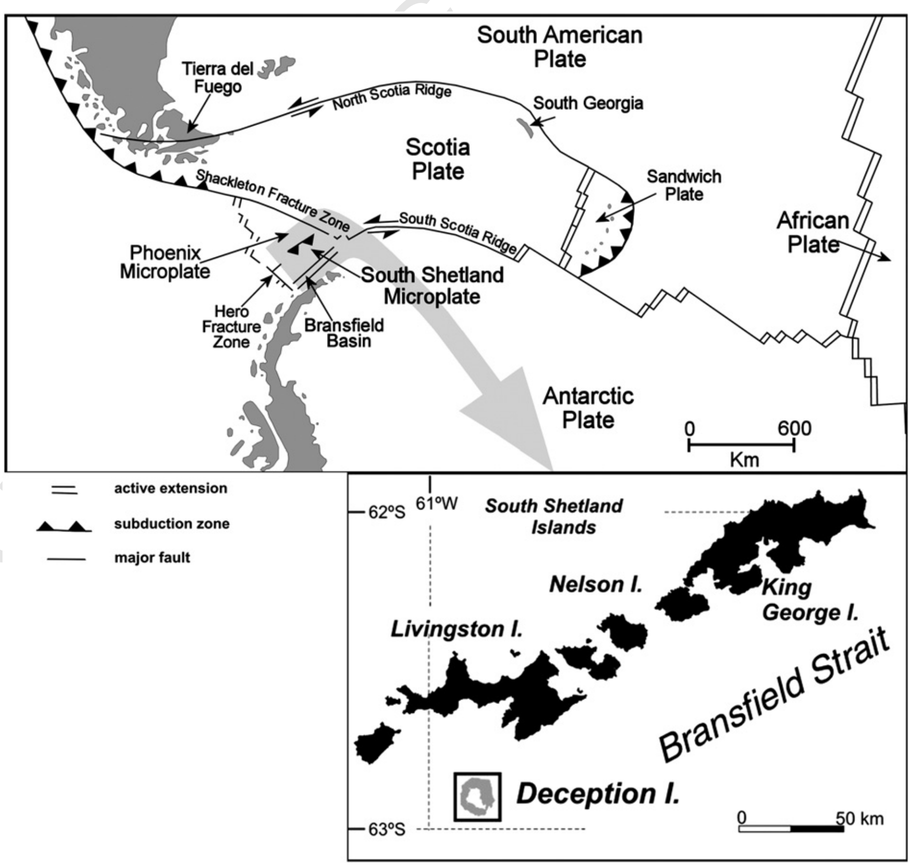

Fig. 1. Regional tectonics and location of Deception Island (South Shetland Islands, Antarctica).

Please cite this article as: Torrecillas, C., et al., Reconstructing palaeo-volcanic geometries using a Geodynamic Regression Model (GRM): Application to Deception Island volcano (Sout..., Geomorphology (2012), http://dx.doi.org/10.1016/j.geomorph.2012.10.032

15 km. The central sector of the island is a sea-flooded caldera depression (Port Foster), with a diameter of 8–10 km connected to the open sea through Neptune's Bellows (Fig. 2).

The morphology of the island exhibits a large variety of landforms and deposits derived from the volcanic activity. Approximately 57% of the surface is covered by glaciers (Smellie et al., 2002). Therefore, the main processes that control the geomorphology of Deception Island are volcanic activity and glacial action. Streams and lakes formed by melting of ice and snow, periglacial activity producing gelifraction, slope processes and the presence of permafrost have also contributed to the evolution of the island's relief (Smellie et al., 2002). The slopes of the outer side of the caldera rim preserve landforms of a pre-caldera edifice, but the original morphology of the caldera is not completely preserved because of marine erosion, collapse of inner flanks, and post-caldera volcanic and hydrothermal activity. The outer perimeter consists mainly of sub-vertical cliffs about 20–40 m high; these are remarkably uniform in height along the northern and western coast (Kendall Terrace) and in the southern area (Cathedral Crags) (Fig. 2). The cliffs show signs of landward retreat caused by sea erosion, with numerous islets, stacking and rocks. The morphology of the surrounding marine shelf indicates an early larger volcano eroded to form an extensive 3–5 km wide submarine platform at depths <100 m on the north and west sides. With respect to glacial geomorphology, the stability of the ice front and ice cover has been influenced by both climate fluctuations and volcanic eruptions (Smellie et al., 2002).

Nearly 60 well-preserved craters, fumaroles, areas of heated ground and deposits from fumarole activity concentrate in the inner sector of the caldera and are associated with the post-caldera volcanic activity (Fig. 2). The most extensive and voluminous flows are located in the north, in Kendall Terrace.

Several hypotheses exist on the shape of Deception Island's before the caldera formation. Hoteldahl (1929) and Olsacher (1956) propose that, before the collapse, there was a single stratovolcano, whilst Hawkes (1961) considers the island a collapsed structure deriving from the subsidence of four pre-existing volcanoes along a ring fracture affecting the underlying basement. Casertano (1963) and Baker et al. (1975) explain the present shape of the island as the result of the collapse of a single volcano, as also Hawkes (1961), but with some parasitic cones in the Neptune Bellows area (see Fig. 3); Birkenmajer (1992) supports the hypothesis of a single volcano with smaller, satellite vents located on its slopes. In contrast Marti and Baraldo (1990), Smellie (2001) and Baraldo et al. (2003) propose a large central stratovolcano with a basement diameter of between 20 and 30 km; their hypothesis is based on the radial distribution of the pre-caldera deposits, as well as multiple small eruptive centres, although they do not fully agree with the polygenetic volcano suggested by Hawkes (1961).

Regarding the formation of the caldera, no geochronological data are available and several hypotheses have been proposed in this respect. The collapse has been attributed to the existence of a large ring fault caused by tangential dislocation and associated radial faults (Olsacher, 1956), or to the presence of various ring-shaped and radial faults (Hoteldahl, 1929; Hawkes, 1961; Birkenmajer, 1992). Smellie (2001) suggests that the edifice collapsed in a major eruption, which reactivated pre-existing structures related to the tectonics of the Bransfield Strait. Vila et al. (1992), Ortiz et al. (1992), Rey et al. (1995) and Garcia et al. (1997) also linked the present-day structure of the island with regional seismic activity generated by a fracture zone in the Bransfield Strait. Baraldo (1999) suggested that the collapse of the central part of the island had its roots in an area of transtension, and compared the collapse to the formation of a 'pull-apart' basin. Marti et al. (1996) rejected the existence of circular and radial faults, and explained the collapse as a reactivation of normal faults orthogonal to the Bransfield Strait extension, following a relatively large eruption in terms of volume ejected.

Great differences, of almost 2000 m, exist regarding the estimated height of the stratovolcano. An altitude of 700–900 m.a.s.l. can be calculated using the data provided by Baker et al. (1975). Birkenmajer (1992) proposed a height of 2500 m.a.s.l., whilst Ben-Zvi et al. (2009) assumed a height of 500 m.a.s.l. in recreating a cone with the material emitted in the great eruption before the collapse.

Post-caldera volcanism on Deception Island mainly developed within the central depression, with small-volume eruptions (about 0.1 km^3 of volcanites between 1956 and 2003, according to Torrecillas et al., 2012) that generated phreatomagmatic and strombolian deposits (Marti et al., 1996; Smellie, 2001). All the exposed post-caldera rocks appear to be late Pleistocene and recent, probably <100 kyr, in age (Shultz, 1970; Smellie, 2001). Recent eruptions (see Fig. 2) since 1842 occurred in the 1829–1912, 1829–1956, 1912–1917 and 1967–1970 periods. All were moderate in magnitude, with small volumes of magma emitted, and of short duration, from a few hours to 2–3 days (Roobol, 1973). Previously, Orheim (1971, 1972) reported between 8 and 33 eruptions during the last 200 years, whilst Björck et al. (1991) refers to 14 eruptions during the last 5 kyr.

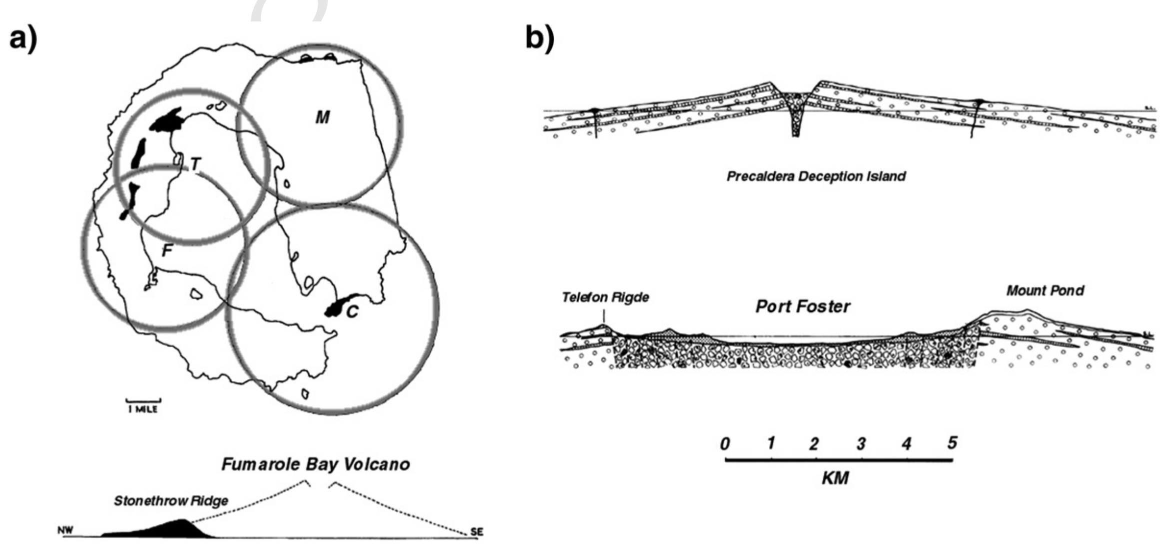

Fig. 2. Morphotectonic elements (Paredes et al., 2007), historical eruptions, names of geographical features and research stations on Deception Island, and pre-caldera deposits according to Smellie et al. (2002).

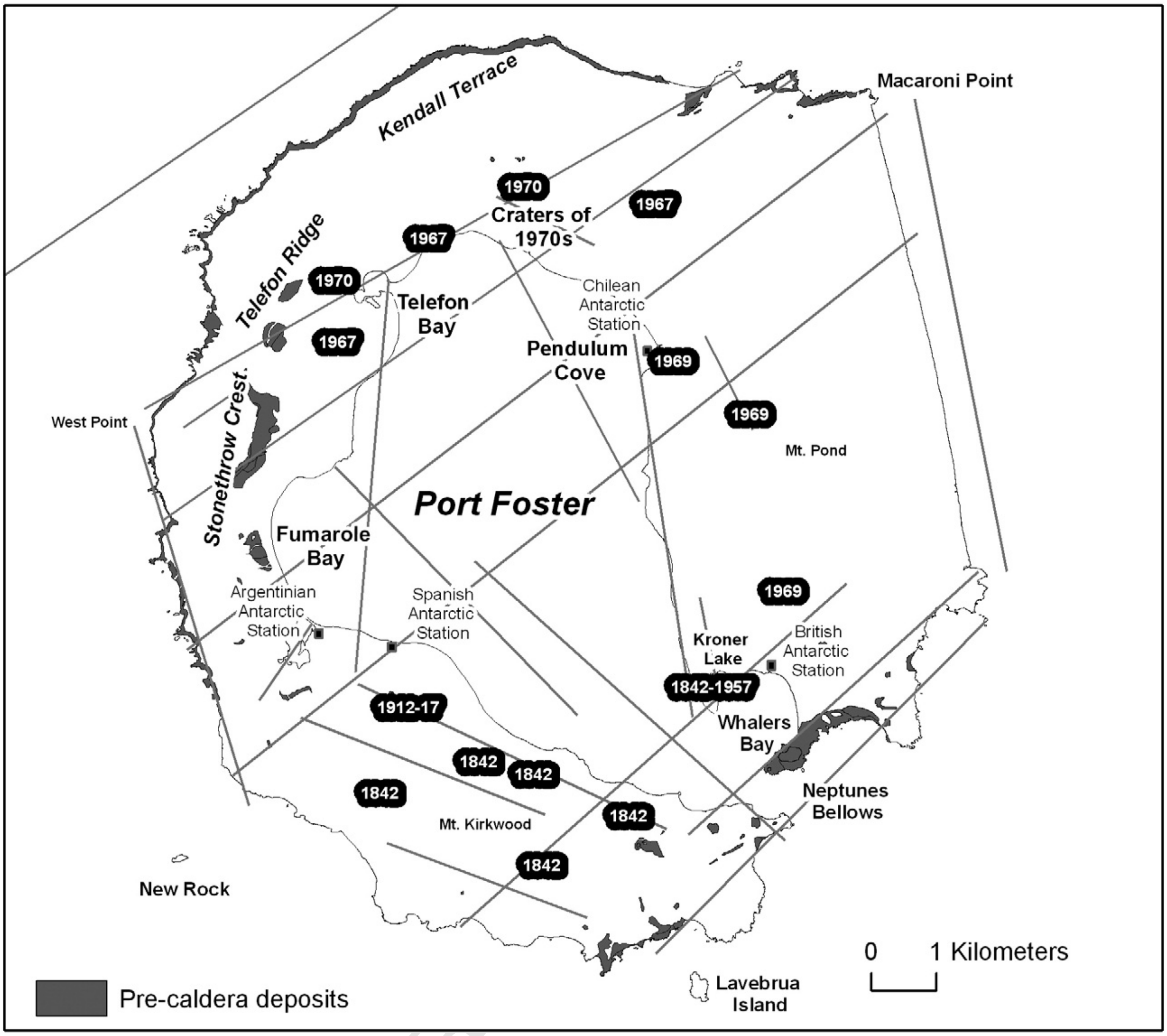

Fig. 3. Geological evolution models. a) Polygenetic volcano model and geological cross-section of Deception Island proposed by Hawkes (1961). b) Theory of Deception Island's evolution according to Baker et al. (1975).

2.1.2. Current palaeo-surface: pre-caldera deposits and palaeo-coastline

The first stage of the methodology proposed here the currently-available data of the palaeo-surface before collapse. The latest published hypothesis on the caldera formation process (Marti et al., 1996; Smellie, 2001) states that it formed by the collapse that followed an eruption of large volume, so the available points of the palaeo-surface are represented by the highest levels of the pre-caldera deposits. The digital geological map, at a 1:25,000 scale (Marti and Baraldo, 1990; Smellie et al., 2002), shows the location of the outcrops of the pre-caldera. First, the pre-caldera deposits were extracted (Fig. 2) and second, a digital topographic map 1:25,000 (SGE, 2006) and its corresponding DEM, with spatial resolution of 2 m, were used to determine the highest elevation of each deposit inside and outside the caldera. The highest points of these deposits on the adjacent islands, Låvebrua and New Rock (Fig. 2) were also included. The elevation of the deposits extracted from this reconstruction represents a minimum estimate because may have been greater in areas where the deposits are not exposed.

Another important item of data on the current surface is the outer shoreline and bathymetry of Deception Island; this is necessary for the determination of the palaeo-coastline. The present coast exhibits a complex evolution, with high lava cliffs rising to a height of over 100 m, and scattered with pre-caldera deposits on the northern and western shorelines; there is a linear coastline due to the action of submarine faulting to the east of the island (Fernandez-Ibañez et al., 2005). There are some adjacent islands which, to judge from their stratigraphic correlation (New Rock Island) or their possible association with a parasitic vent (Låvebrua Island) (Birkenmajer, 1992), must have once been part of Deception Island itself.

The first geometric approximation of the palaeo-coastline is the graphic proposed from Baraldo's hypothesis for the formation of the island with a stratovolcano and several parasitic volcanoes (Baraldo, 1999), see Fig. 4. With the aim of improving this geometry, the extrapolation of the dips of the pre-caldera deposits from the digital geomorphological map (Smellie et al., 2002) to bring the surface closer to sea level was considered. Only six dip values are near the coastline. Then an exterior bathymetry of the island (scale 1:500,000) in raster format (Barclay et al., 2009), in an attempt to find the shape near the location of the volcanoes that predated the collapse (scale 1:200,000), as proposed by Baraldo (1999) (Fig. 4), including the adjacent islands was considered. The initial selection was the −100 m bathymetry, although this has to be interpolated in zones where no

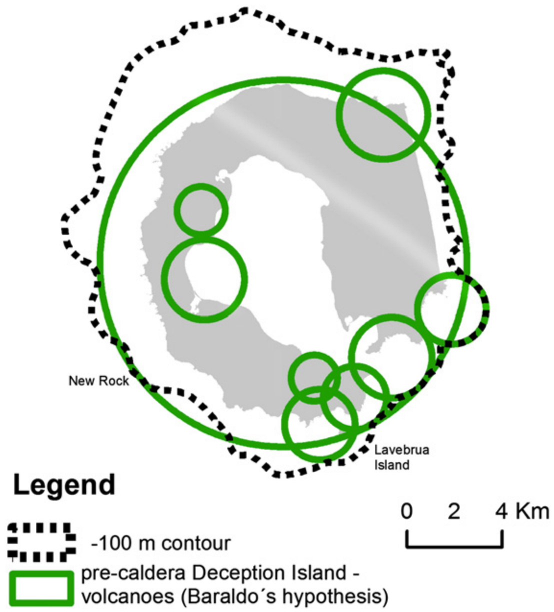

Fig. 4. Baraldo's hypothesis for the formation of the island (Baraldo, 1999), with the defined palaeo-coastline partly coinciding with the −100 m bathymetric curve (Barclay et al., 2009), extended in the southern zone to cover the limits of the parasitic volcanoes.

information is available; and in the south and east of the island, the curve is extended slightly to include some of the boundaries of the parasitic volcanoes.

2.1.3. Current palaeo-surface: location and height of the stratovolcano

An attempt was made to define the pre-caldera edifice by studying the actual topography of the island. With that aim, four possible planimetric locations of the summit were selected based on geometric criteria. The four centres considered are the geometric centres 1 of the present dividing line (cD); 2 of the outer coast (cOC); 3 of the inner coastline (cIC), and 4 of the deepest (−170 m) bathymetry of the inner bay (cB). As can be observed in Fig. 5a, cD, cOC and cIC are very close each other, so it was decided to take their arithmetic mean value (cM) and then study only two points (cB and cM).

The radial slopes extrapolated from these possible summit locations were then studied. Starting from these two points (cB and cM), eight radial profiles were selected to compute the mean slope, which was then extrapolated, in both cases, to find the point of intersection, over Port Foster, that is taken as one possible location of the central peak. This methodology has been widely used previously, for example by Hildebrand et al. (2008, Fig. 5). As the Deception Volcano is an island with high cliffs along its coastline, the mean slope computed with the present topography is not very representative, so it was decided to consider the mean slope closer to the highest point of each profile. Fig. 5b shows the planimetry of the profiles considered with a line joining the summit of each profile for the two centres and two cases of slopes studied, mean slope and the mean slope closer to the highest point. The possible planimetric locations of the summit tend to be in the south, with only six points out of the total of thirty two in the north. This may indicate the location in the southern zone of the parasitic volcanoes that several authors hypothesised (Casertano, 1963; Baker et al., 1975; Marti and Baraldo, 1990; Birkenmajer, 1992; Smellie, 2001; Baraldo et al., 2003), in view of the fact that the mean slope value is higher in the south, corresponding with a rough relief. It was decided to eliminate profiles running N–S and NNE–SSE to reduce this possible influence of the parasitic volcanoes. The mean location of summit is $x = 619{,}309$ m, $y = 3{,}015{,}645$ m and $z = 1267$ m.a.s.l, in UTM projection, zone 20S and geodetic system WGS84, with standard deviations of $\sigma_x = \pm 1431$ m, $\sigma_y = \pm 1348$ m and $\sigma_z = \pm 413$ m. This is at a distance of 1200 m from the planimetric location proposed by Baraldo (1999), and falls within the margin of error in location.

With respect to the height, the values proposed by previous authors should be recalled: 700–900 m.a.s.l by Baker et al. (1975), 2500 m.a.s.l. by Birkenmajer (1992) and 500 m.a.s.l. by Ben-Zvi et

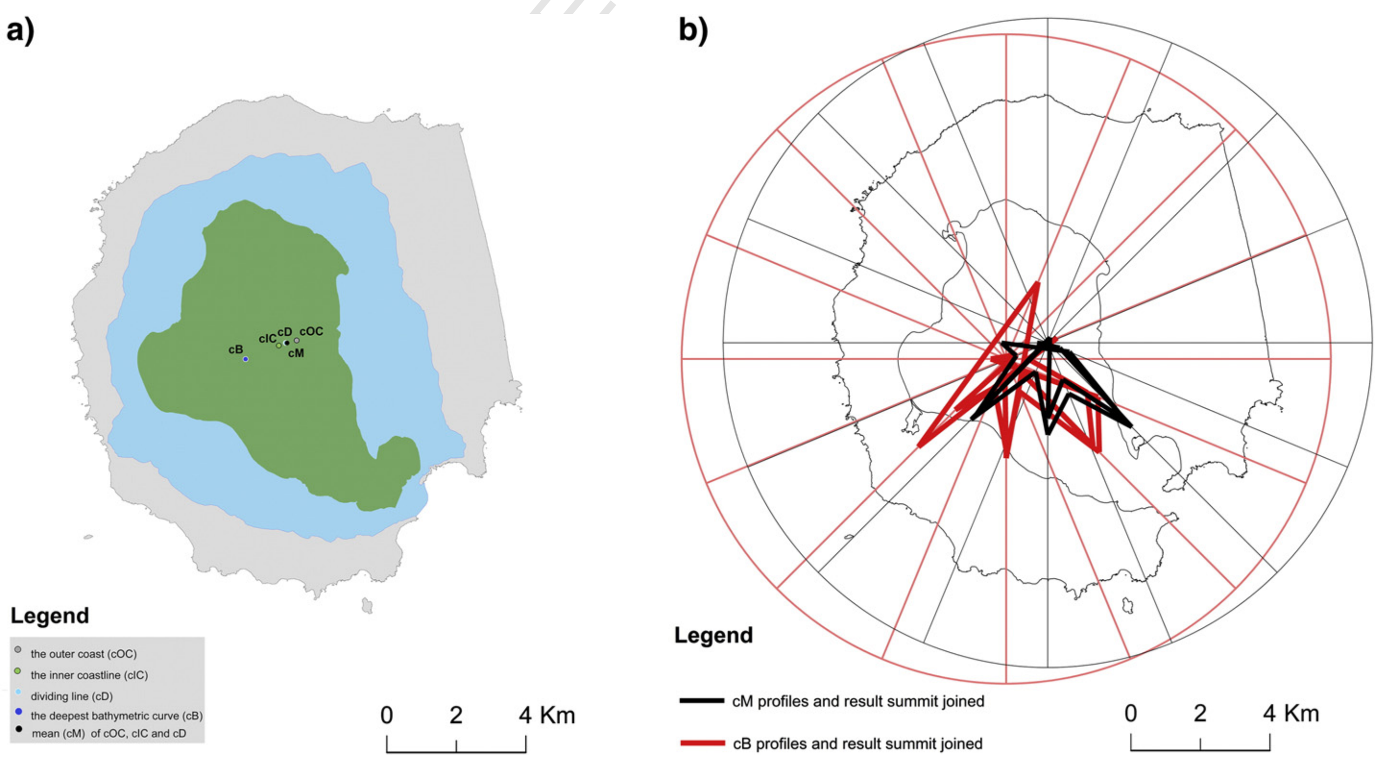

Fig. 5. a) Geometric centres on the island initially studied as possible palaeo-summits; b): The figure obtained by joining 1) the summit elevations given by the profiles from the midway point between the coast and the caldera (cM) and 2) the centre of the bathymetric curve (cB).

Please cite this article as: Torrecillas, C., et al., Reconstructing palaeo-volcanic geometries using a Geodynamic Regression Model (GRM): Application to Deception Island volcano (Sout..., Geomorphology (2012), http://dx.doi.org/10.1016/j.geomorph.2012.10.032

al. (2009). The only value that agrees with the height obtained in the present study, and its standard deviation, is that of Baker et al. (1975).

2.1.4. GRM: geometric transformation

In this second stage, the digital tectonic model of the area, the local deformation of the Island obtained by Berrocoso et al. (2008), and the digital morphotectonic alignments (scale 1:25,000, Paredes et al., 2006, 2007; Perez-Lopez et al., 2007), see Fig. 2, were used. The other main parameter is the past date; the period of regression selected was 100 kyr (Smellie, 2001), corresponding with the dating of the oldest rock before the formation of the caldera (carried out by Shultz, 1970): hence the most recent date estimated for that event.

Deception Island is located at the north-western end of the expansion axis of the Central Bransfield Basin; its superficial deformation is due to expansion of the Bransfield Rift (Gracia et al., 1996; Barker et al., 2003; Berrocoso et al., 2008), with superimposed local effects due to caldera collapse and magmatic activity (Vila et al., 1992; Berrocoso et al., 2008).

Gonzalez-Ferran (1991) suggested a mean value for the Bransfield Rift expansion of 2.5–7.5 mm/yr in the NW–SE direction for the last 2 Myr. More recently, Dietrich et al. (2004) indicated a general value for this displacement of ~10 mm/yr in the NE–SW direction for South Shetland Islands; and the research group led by Prof. Berrocoso estimates a global horizontal mean displacement 20.5 mm/yr from 1999 to 2009 in Deception Island, in the same direction as Dietrich et al. (2004), both using Global Positioning system (GPS) data. Although Gracia et al. (1996, Fig. 5) show strike directions of fault scarps in the Central Bransfield Basin, where Deception Island is located, in both directions, NE–SW and NW–SE, the number of faults in the latter direction is one order of magnitude lower than in the former. It is therefore possible that, over the years since the formation of the caldera, the general direction of displacement has been the present-day NE–SW direction, but always of less magnitude than the NW–SE displacement.

Regarding local deformation, Perez-Lopez et al. (2007) proposes the existence of the same two main directions of deformation to explain the elliptical form of the caldera's lip. Geodetic studies carried out between 1987 and 2011 by Berrocoso's team also computed deformation models for Deception Island, without any regional displacement of South Shetland Island; horizontal deformation rates up to 40 mm/yr were obtained in 1989–96 at the GPS stations of BARG and FUMA (Ramirez et al., 2008); these models confirm the two main directions of extension of the Bransfield Rift (NW–SE and NE–SW) as the directions of local deformation (see Fig. 6, for 2002–2003). In the last 20 years, the local deformation can be quantified, with values of 15 mm/yr for NE–SW, and 5 mm/yr for NW–SE. Although 20 years of deformation study are not significant on a time scale of 100 kyr, these values and directions are in accordance with the morpho-structural evolution of the Central Bransfield Basin presented by Gracia et al. (1996, Fig. 10), where the NE–SW deformation direction is predominant over the NW–SE one. Therefore, these conservative values as input parameter for our GRM were taken.

Taking into account the combined regional and local geodynamic deformation, a geodynamic regression model (GRM) with a planimetric transformation for a period of 100 kyr using values of 1.5 km (NE–SW) and 0.5 km (NW–SE) was applied.

This transformation converts an approximate circle to an approximate ellipse due to differences in the values for the two directions, and has been applied to the current palaeo-coastline, to the pre-caldera deposits points, to the circular limits of Baraldo's parasitic volcanoes, and to the centre of the main volcano (Fig. 7). After transformation, the circular boundaries of Baraldo's parasitic volcanoes became ellipses, but after applying the value of the semi-major axis, they recovered their circular shape. Although this final shape obtained for the palaeo-coastline is not approximately circular, by the date of reconstruction selected (100,000 years ago) this volcano was already some 600,000 years old, according to the estimates of its date of initial formation, and so some of its original circularity could have been lost. The presence of parasitic volcanoes could also modify the final shape.

2.1.5. GRM: recalculated heights of the main volcano and parasite cones

The summit height calculated in the first stage has an elevation error of $\sigma_z = \pm 413$ m; taking this into account, the maximum height estimated for the Deception Island volcano is 540 m. It was decided to re-calculate the summit height with the palaeo-boundary data and the spot heights obtained from the GRM in an initial interpolation of the island's topography, but only up to the lip of the caldera. This was done using the Topogrid method, an iterative finite difference method based on a thin-plate spline technique, using ESRI's ArcGIS™ software (version 10). Eight profiles were studied: two oriented along the main deformation axes and six others. Extrapolating the maximum final slope of each profile, a mean value of 580 m ± 62 m (Fig. 8) was obtained; accepting this uncertainty, this value is taken as the height of the original stratovolcano.

Taking into account the mass balance due to ice, Orheim (1972, p.7) defines a current equilibrium line at between 200 and 250 m, with accumulation zones of more than 40 m. The last glaciation began approximately 100 kyr ago (Newnham et al., 1999), so the mass of snow and ice had to be considered, and the value of the definitive height needs to be increased. By raising the altitudes by values of between 200 and 250 m, the mean slope changes, and the summit height increases. From the profiles, a mean increase of 70 ± 30 m is determined for the summit height, and this is then rounded off to 650 m.

Before the final interpolation, it was necessary to determine the height of the proposed parasitic volcanoes. To do this, data on the elevation of the pre-caldera deposits located within the limit of each initial volcano were used as minimum height. To calculate the summit heights of the parasitic cones, a slope of 10° is considered, which corresponds to the mean slope of Deception Island's palaeo-volcano and to the current mean slope.

2.1.6. GRM: interpolation, sea level and virtual model

Final values for the pre-caldera topography have been calculated using a two-stage process of interpolation. First, the principal stratovolcano was reconstructed, and then the adjacent parasite volcanoes were added. The Topogrid method was used for both the interpolations. The first interpolation shows irregular small mounds in the southern zone; these forms were interpreted as parasitic vents existing in the areas presently known as Neptune's Bellows and Macaroni Point. In the second interpolation these mounds were replaced by parasitic volcanoes.

Before stating the definitive volume and perimeter values obtained, it is worth looking at one more factor of potential influence on our reconstruction: Antarctic sea level trends for the Holocene–Late Pleistocene. For King George Island, which also belongs to the South Shetland archipelago, around 40 kyr ago, Nakada et al. (2000) estimated a value of 10 m above the present sea level. In the Vestfold Hills, East Antarctica, Zwartz et al. (1998) proposed values ranging from 7.5 m (8000 years ago) to a 9 m above the present sea level (6.2 kyr ago). Rohling et al. (2009) estimated the sea level for the Middle Pliocene epoch (3.0–3.5 Myr) at 25 ± 5 m above the present level in Antarctica, presenting a study of this period which included periodic cycles when the sea level rose above present-day levels. The graphic material presented by Rohling et al. (2009) corresponding to 100 ± 5 kyr ago, shows relative sea levels between 0 and 40 m.

As a conservative value, it was decided to take the value given by Nakada et al. (2000) for the geographic zone closest to Deception Island, and the upper sea level height used in the proposed model was reduced by 10 m to obtain the final result.

The change in sea level reduced the estimated emerged stratovolcano volume by 1 km^3, leaving the final palaeo-volume at 19.6 km^3,

Please cite this article as: Torrecillas, C., et al., Reconstructing palaeo-volcanic geometries using a Geodynamic Regression Model (GRM): Application to Deception Island volcano (Sout..., Geomorphology (2012), http://dx.doi.org/10.1016/j.geomorph.2012.10.032

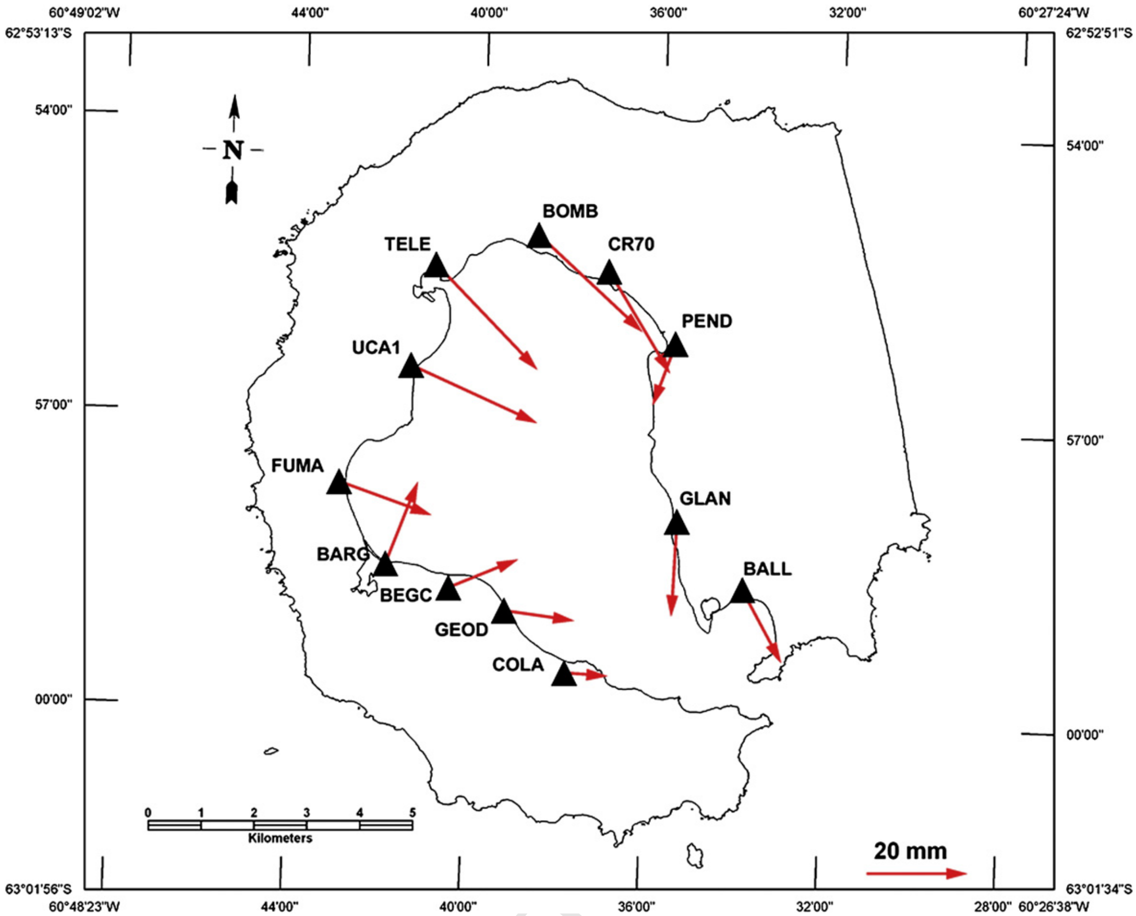

Fig. 6. Horizontal displacement rates of surface deformation values for the period 2002–2003 at several points of the deformation control network on Deception Island.

as opposed to the present-day volume of 15.7 km^3. In the reconstruction, the palaeo-surface area is 104.8 km^2 compared with the present-day area of 96 km^2; the perimeter is 42 km compared to the present outer perimeter of 57 km (excluding the internal coastline). This value of the perimeter has been obtained from a map at a scale of 1:100,000, and these values are partly the result of including Port Foster. The height of the volcano is also affected, so the final palaeo-volcanic summit height takes a definitive value of 640 m. Fig. 9a shows the palaeo-DEM with the current coastline, and, in Fig. 9b and c, two 3D views. In Fig. 10a and b there are two photorealistic images of the island obtained by superposition over the palaeo-surface of textures extracted from the 2003 Panchromatic

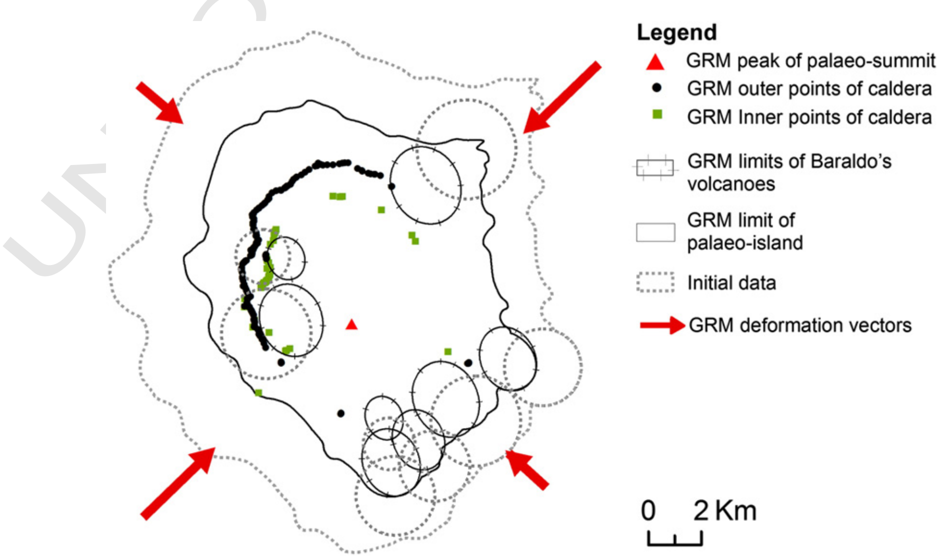

Fig. 7. Result of applying the Geodynamic Regression Model to pre-caldera deposits, Baraldo's parasite volcanoes and palaeo-coastline, the latter with new sizes after reshaping them as circles using the semi-major axis value as radius value.

Please cite this article as: Torrecillas, C., et al., Reconstructing palaeo-volcanic geometries using a Geodynamic Regression Model (GRM): Application to Deception Island volcano (Sout..., Geomorphology (2012), http://dx.doi.org/10.1016/j.geomorph.2012.10.032

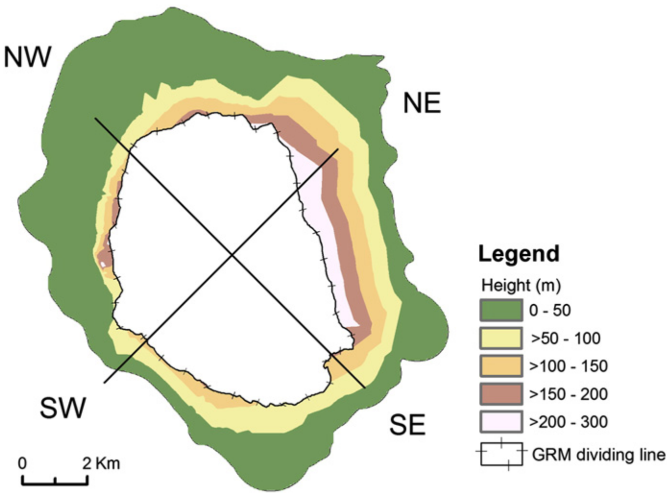

Fig. 8. DEM resulting from the interpolation of data, with the subsequent elimination of the caldera, to calculate a possible summit height, and location of main profiles used to determine a palaeo-summit.

Quick Bird satellite image of the island and photographs. For the sake of greater realism, the summit peak has been replaced by a ring.

3. Summary and conclusions

The morphology of a volcano is obviously influenced by the eruptive activity but geodynamics and volcanic deformation may also contribute. The diversity of methodologies proposed by various authors for the reconstruction of palaeo-volcanic surfaces indicates that a standard procedure is still lacking. Significantly, the methodologies previously proposed do not take into consideration geodynamics and superficial deformation parameters, as well as differences in sea level or mass balance due to ice. A volcanic reconstruction method is proposed which differs from the other ones because it includes the Geodynamic Regression Model (GRM) and takes into account the tectonic and volcanic deformation. There are two stages in the GRM approach proposed here. The objective in the first stage is to obtain the palaeo-surface from the existing remains and from existing hypotheses of the particular volcano's evolution. In the second stage, deformations are included and deformation vectors are defined. The palaeo-surface is obtained with a geometric transformation. If the volcano's height is not considerably above the sea level or it is affected by permanent ice and snow, the influence of these factors on the height must be evaluated.

In the reconstruction present here, the influence of the GRM on the final shape of Deception Island volcano is verified. Although this final shape is not approximately circular, which is the normal shape in most volcanoes, by the selected time of reconstruction (100 kyr ago) this volcano was already some 700,000 years old, according to the age estimates, and some of its original circularity could have been lost. The final surface reveals the existence of early parasitic volcanoes with altitudes of much less than 650 m in the locations presently known as Neptune's Bellows and Macaroni Point.

A pre-collapse 100 kyr time period age was selected for the reconstruction of the Deception Island palaeo-edifice. The results show an old stratovolcano with a perimeter slightly less than 42 km and a volume of 19.6 km^3. With respect to the palaeo-summit height, our initial value of 580 m (with $\sigma_z = \pm 62$ m) was modified to 640 m by taking into account the estimated changes in the sea level and the mass of ice and snow cover. A new value for σ_z has been estimated at about $\pm$100 m because of the influence of the snow has an error of $\pm$30 m and the palaeo-sea level error is unknown.

The accuracy of this reconstruction depends on the degree of degradation of the volcanic flanks and on the knowledge of the volcano's evolution. The geological evolution of Deception Island is not clear, and the relicts of the palaeo-volcano are scarce due to more recent volcanic activity.

The main outcome of our study is that GRM method can be applied to other scenarios provided that reliable local deformation data are available.

4. Uncited reference Q2

Orheim, 1975

Acknowledgements

This geodetic research has been carried out with the support of the Spanish Ministry of Education and Science as part of the National Antarctic Program. To date, the following research projects have been

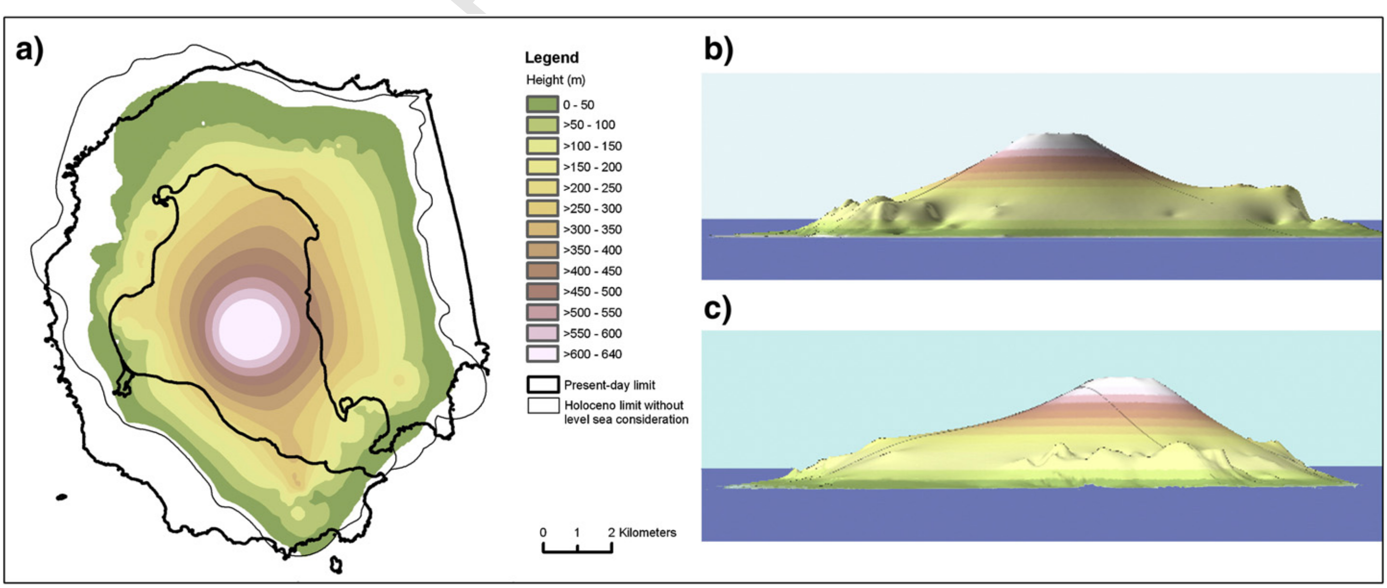

Fig. 9. a) Deception Island DEM before caldera formation with superposition of present-day limit and Holocene limit without considering differences in sea level, b) 3D view from the E with 3× exaggeration in Z and c) 3D view from the NW with 3× exaggeration in Z.

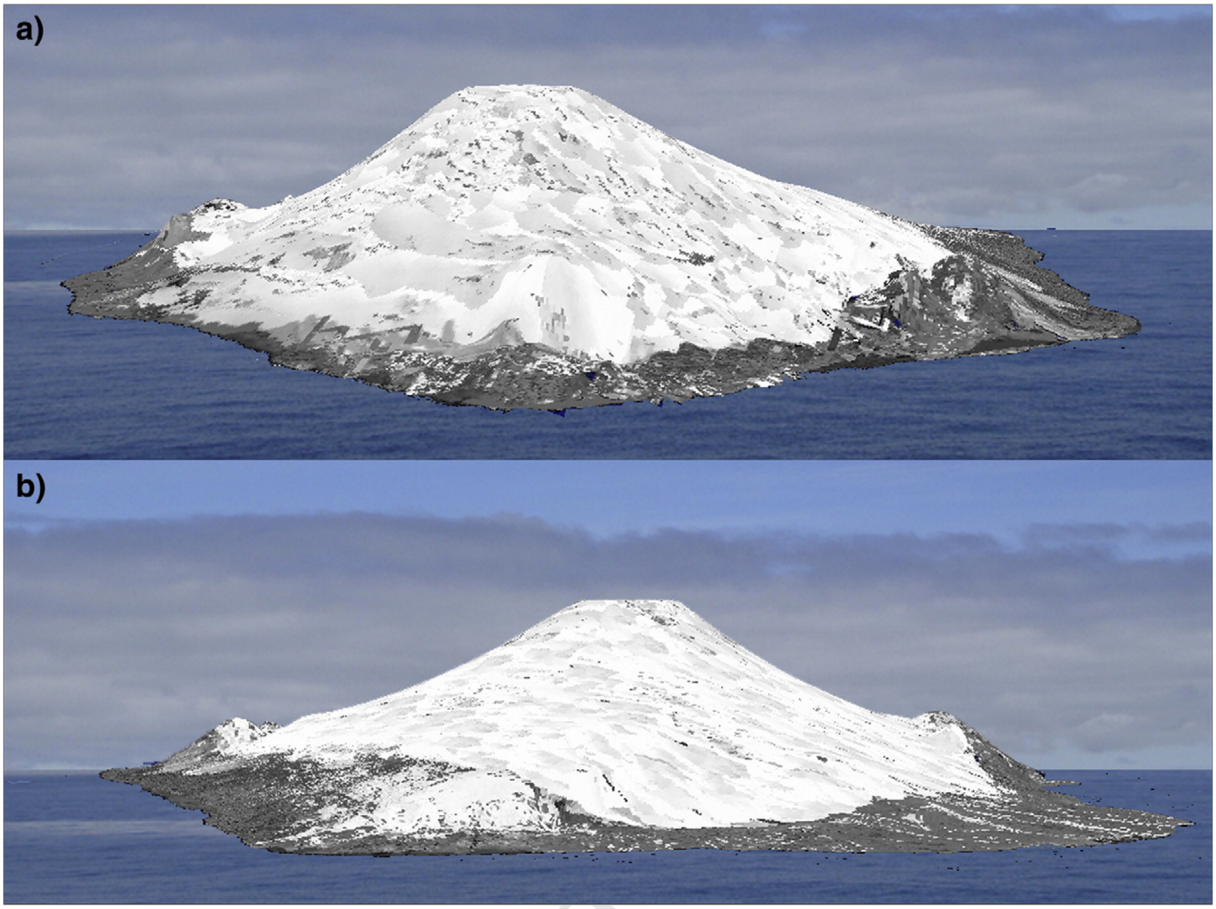

Fig. 10. Photorealistic images of the island obtained by superposition of textures extracted from the Quick Bird satellite image over the palaeo-reconstruction obtained in this study, with 3× exaggeration in Z: a) 3D view from N; and b) 3D view from W.

awarded: "Geodetic Studies on Deception Island: deformation models, geoid determination and Scientific Information System (REN2000.0551.C03.01/ANT)"; "Geodetic Control of the volcanic activity of Deception Island (CGL2004.21547.E/ANT)"; "Update of the Spanish Cartography for Deception Island (CGL2004.20408.E/ANT)"; "Volcano-tectonic activity on Deception Island: geodetic, geophysical investigations and Remote Sensing on Deception Island and its surroundings (CGLl2005-07589-c03-01/ANT)"; "Geodetic Control of the volcanic activity on Deception Island (CONGEODEC, CGL2004-21547-E)"; and "Geodetic and geothermic investigations, time-frequency analysis and volcanic innovation in Antarctica (South Shetland Islands — Antarctic Peninsula) (GEOTINANT, CTM2009-07251)". The authors thank Dr. Jose Manuel Marrero, for his comments on an earlier version of this manuscript, and are grateful to Professor Guido Ventura and an anonymous referee for their helpful comments and suggestions.

Most of the data used have been taken from an existing multi-disciplinary geographic information system about the island known as SIMAC (Torrecillas Lozano et al., 2006), which has a dedicated web site, SIMACWEB (http://simac.uca.es).

References

Baker, P., Roobol, M., McReath, M., Harvey, M., Davies, T., 1975. The geology of the South Shetland Islands. Volcanic evolution of Deception Island: introduction. British Antarctic Survey, Scientific Reports 78, 3–15.

Baraldo, A., 1999. Evolucion geologica de la isla Decepcion, islas Shetland del Sur, Antartida. Ph.D.Thesis. Departamento de Ciencias Geologicas. Universidad de Buenos Aires, Argentina. 213 pp.

Baraldo, A., Papalini, A.E., Böhnel, H., Mena, M., 2003. Paleomagnetic study of Deception Island, South Shetland Islands, Antarctica. Geophysical Journal International 153, 333–343.

Barclay, A.H., Wilcock, W.S.D., Ibañez, J.M., 2009. Bathymetric constraints on the tectonic and volcanic evolution of Deception Island Volcano, South Shetland Islands. Antarctic Science 21, 153–167.

Barker, D., Christeson, G., Austin, J., Dalziel, I., 2003. Backarc basin evolution and cordilleran orogenesis: insights from new ocean-bottom seismograph refraction profiling in Bransfield Strait, Antarctica. Geology 31, 107–110.

Ben-Zvi, T., Wilcock, W.S.D., Barclay, A.H., Zandomeneghi, D., Ibañez, J.M., Almendros, J., 2009. The P-wave velocity structure of Deception Island, Antarctica, from two-dimensional seismic tomography. Journal of Volcanology and Geothermal Research 180, 67–80.

Berrocoso, M., Fernandez-Ros, A., Ramirez, M.E., Salamanca, J.M., Torrecillas, C., Perez-Peña, A., Paez, R., Garcia-Garcia, A., Jimenez-Teja, Y., Garcia-Garcia, F., Soto, R., Garate, J., Martin-Davila, J., Sanchez-Alzola, A., de Gil, A., Fernandez-Prada, J.A., Jigena, B., 2008. Geodetic Research on Deception Island and its Environment (South Shetland Islands, Bransfield Sea and Antarctic Peninsula) During Spanish Antarctic Campaigns (1987–2007). Geodetic and Geophysical Observations in Antarctica. Springer-Verlag, Berlin, Heidelberg, pp. 97–124.

Birkenmajer, K., 1992. Volcanic succession at Deception Island, West Antarctica: a revised litho-stratigraphic standard. Studia Geologica Polonica 101, 27–82.

Björck, S., Sandgren, P., Zale, R., 1991. Late Holocene tephrochronology of the northern Antarctic Peninsula. Quaternary Research 36, 3322–3328.

Casertano, L., 1963. Volcanic activity at Deception Island. Proceedings of the First International SCAR-IUGS Symposium on Antarctic Geology (Cape Town, South Africa). Geomorphology 2, 33–47.

Coleman, M.L., Niemann, J.D., Jacobs, E.P., 2009. Reconstruction of hillslope and valley paleotopography by application of a geomorphic model. Computers and Geosciences 35, 1776–1784.

Dietrich, R., Rülke, A., Ihde, J., Lindner, K., Miller, H., Niemeier, W., Schenke, H., Seeber, G., 2004. Plate kinematics and deformation status of the Antarctic Peninsula based on GPS. Global and Planetary Change 42, 313–321.

Fernandez-Ibañez, F., Perez-Lopez, R., Martinez-Diaz, J.J., Paredes, C., Giner-Robles, J.L., Caselli, A.T., Ibañez, J.M., 2005. Costa Recta beach, Deception Island, West Antarctica: a retreated scarp of a submarine fault? Antarctic Science 17, 418–426.

Garcia, A., Blanco, I., Torta, J.M., Astiz, M.M., Ibañez, J.M., Ortiz, R., 1997. A search for the volcanomagnetic signal at Deception volcano (South Shetland Islands, Antarctica). Annali di Geofisica 40, 319–327.

Gonzalez-Ferran, O., 1991. The Bransfield rift and its active volcanism. In: Thomson, R.A., Crame, J.A., Thomson, J.W. (Eds.), Geological Evolution of Antarctica. Cambridge University Press, Cambridge, pp. 505–509.

Gracia, E., Canals, M., Farran, M., Prieto, M.J., Sorribas, J., Team, Gebra, 1996. Morphostructure and evolution of the Central and Eastern Bransfield Basins (NW Antarctic). Marine Geophysical Research 18, 429–448.

Hawkes, D.D., 1961. The geology of the South Shetland II. The geology and petrology of Deception Island. British Antarctic Survey. Falkland Island Dependences Survey Scientifics Reports 27, 1–43.

Hildenbrand, A., Gillot, P., Marlin, C., 2008. Geomorphological study of the long-term erosion on a tropical volcanic ocean island: Tahiti-Nui (French Polynesia). Geomorphology 93, 460–481.

Hoteldahl, O., 1929. On the geology and physiography of some Antarctic and Sub-Antarctic Islands. Scientific results of the Norwegian Antarctic Expedition 1927–1928 and 1928–1929. I Kommisjon Hos Jacob Dybwadf, Oslo. (172 pp.).

Isaia, R., D'Antonio, M., Dell'Erba, F., Di Vito, M., Orsi, G., 2004. The Astroni volcano: the only example of the closely-spaced eruptions in the same vent area during the recent history of the Campi Flegrei caldera (Italy). Journal of Volcanology and Geothermal Research 133, 171–192.

Marti, J., Baraldo, A., 1990. Pre-caldera pyroclastic deposits of Deception Island (South Shetland Islands). Antarctic Science 2, 345–352.

Marti, J., Vila, J., Rey, J., 1996. Deception Island (Bransfield Strait, Antarctica): an example of a volcanic caldera developed by extensional tectonics. In: McGuire, W.J., Jones, A.P., Neuberg, J. (Eds.), Volcano Instability on the Earth and Other Planets, Geological Society Special Publication No.110. Geological Society of London, London, pp. 253–265.

Nakada, M., Kimura, R., Okuno, J., Moriwaki, K., Miura, H., Maemoku, H., 2000. Late Pleistocene and Holocene melting history of the Antarctic ice sheet derived from sea-level variations. Marine Geology 167, 85–103.

Newnham, R.M., Lowe, D.J., Williams, P.W., 1999. Quaternary environmental change in New Zealand: a review. Progress in Physical Geography 23, 567–610.

Olsacher, J., 1956. Contribucion a la geologia de la Antartida Occidental y contribucion al conocimiento de la Isla Decepcion. Publicacion del Instituto Antartico Argentino 2, 25–76.

Orheim, O., 1971. Volcanic activity on Deception Island, South Shetland Island. In: Adie, R.J. (Ed.), Antarctic Geology and Geophysics. Universitetsforlaget, Oslo, pp. 117–120.

Orheim, O., 1972. A 200-year record of glacier mass balance at Deception Island Southwest Atlantic Ocean, and its bearing on models of global climatic change. Inst. Polar Studies, Ohio State University Columbus, Report (118 pp.).

Orheim, O., 1975. Past and present mass balance variations and climate at Deception Island, South Shetland Islands, Antarctica. Snow and Ice Symposium — Neiges et Glaces, Moscow. International Association of Hydrological Sciences Publication 104, 161–180.

Ortiz, R., Vila, J., Garcia, A., Camacho, A.G., Diez, J.L., Aparicio, A., Soto, R., Viramonte, J.G., Risso, C., Menegatti, N., Petrinovic, I., 1992. Geophysical features of Deception Island. In: Yoshida, Y., Kaminuma, K., Shiraishi, K. (Eds.), Recent Progress in Antarctic Earth Science. Terra Scientific Publishing Company, Tokyo, pp. 443–448.

Paredes, C., Perez-Lopez, R., Giner-Robles, J.L., De la Vega, R., Garcia-Garcia, A., Gumiel, P., 2006. Distribucion espacial y zonificacion tectonica de los morfolineamientos en la Isla Decepcion (Shetland del Sur, Antartida). Geogaceta 39, 75–78.

Paredes, C., De la Vega, R., Perez-Lopez, R., Giner-Robles, J.L., Martinez-Diaz, J.J., 2007. Descomposicion fractal en subdominios morfotectonicos del mapa de lineamientos morfologicos en la isla Decepcion (Shetland del Sur, Antartida). Boletin Geologico y Minero 118, 775–787.

Perez-Lopez, R., Giner-Robles, J.L., Martinez-Diaz, J.J., Rodriguez-Pascua, M.A., Bejar, M., Paredes, C., Gonzalez-Casado, J.M., 2007. Upper Crustal Structure of Deception Island Area, Bransfield Strait, West Antarctica. USGS Open File Report. U.S. Geological Survey and the National Academies; USGS OFR-2007-1047, Short Research Paper 086.

Ramirez, M.E., Berrocoso, M., Gonzalez, M.J., Fernandez, A., 2008. Crustal Deformation Models and Time-Frequency Analysis of GPS Data from Deception Island Volcano (South Shetland Islands, Antarctica). In: Donner, R.V., Barbosa, S.M. (Eds.), Nonlinear Time Series Analysis in the Geosciences, Lecture Notes in Earth Sciences. Springer-Verlag, Berlin, Heidelberg, pp. 245–272.

Rey, J., Somoza, L., Martinez-Frias, J., 1995. Tectonic, volcanic and hydrothermal event sequence on Deception Island (Antarctica). Geo-Marine Letters 15, 1–8.

Rodriguez, O., Obando, M., Castillo, L., Cepeda, H., 2004. Pyroclastic flow modeling to reconstruct a volcanic edifice in Paipa (Boyaca — Colombia). Earth Science Research Journal 8, 56–62.

Rodriguez-Gonzalez, A., Fernandez-Turiel, J.L., Perez-Torrado, F.J., Gimeno, D., Aulinas, M., 2010. Geomorphological reconstruction and morphometric modelling applied to past volcanism. International Journal of Earth Sciences 99, 645–660.

Rohling, E.J., Grant, K., Bolshaw, M., Roberts, A.P., Siddall, M., Hemleben, Ch., Kucera, M., 2009. Antarctic temperature and global sea level closely coupled over the past five glacial cycles. Nature Geoscience 2, 500–504.

Roobol, M.J., 1973. Historic volcanic activity at Deception Island. British Antarctic Survey Bulletin 32, 23–30.

SGE, Servicio Geografico del Ejercito Español, 2006. New Topographic map of Deception Island 1:25,000. Madrid, Spain.

Shultz, C.H., 1970. Petrology of the Deception Island volcano, Antarctica. Antarctic Journal U.S. 5, 97–98.

Smellie, J.L., 2001. Lithostratigraphy and volcanic evolution of Deception Island, South Shetland Islands. Antarctic Science 13, 188–209.

Smellie, J.L., Lopez-Martinez, J., Headland, R.K., Hernandez-Cifuentes, F., Maestro, A., Miller, I.L., Rey, J., Rey, J., Serrano, E., Somoza, L., Thomson, J.W., 2002. Geology and Geomorphology of Deception Island. BAS GEOMAP SERIES, Sheet 6A and 6B. British Antarctic Survey. (77 pp.).

Szekely, B., Karatson, D., 2004. DEM-based morphometry as a tool for reconstructing primary volcanic landforms: examples from the Borzsony Mountains, Hungary. Geomorphology 63, 25–37.

Torrecillas Lozano, C., Berrocoso Dominguez, M., Garcia Garcia, A., 2006. The Multidisciplinary Scientific Information Support System (SIMAC) for Deception Island, Antarctica. Contributions to Global Earth Sciences. Springer-Verlag, Berlin, Heidelberg, pp. 397–402.

Torrecillas, C., Berrocoso, M., Perez-Lopez, R., Torrecillas, M.D., 2012. Determination of volumetric variations and coastal changes due to historical volcanic eruptions using historical maps and remote-sensing at Deception Island (West Antarctica). Journal of Geomorphology 136, 6–14.

Vila, J., Ortiz, R., Correig, A., Garcia, A., 1992. Seismic activity on Deception Island. In: Yoshida, Y., Kaminuma, K., Shiraischi, K. (Eds.), Recent Progress in Antarctic Earth Science. Terra Scientific Publishing Company, Tokyo, pp. 449–456.

Vogel, S., Marker, M., 2010. Reconstructing the Roman topography and environmental features of the Sarno River Plain (Italy) before the AD 79 eruption of Somma-Vesuvius. Geomorphology 115, 67–77.

Zwartz, D., Bird, M., Stone, J., Lambeck, K., 1998. Holocene sea-level change and ice-sheet history in the Vestfold Hills, East Antarctica. Earth and Planetary Science Letters 155, 131–145.